

https://doi.org/10.1070/QEL17981

Radiation source based on an optical parametric oscillator with MgO:PPLN crystal and volume Bragg grating, tunable in ranges of 2050–2117 and 2140–2208 nm

N.Yu. Kostyukova, E.Yu. Erushin, A.A. Boyko, D.B. Kolker

Abstract. **A tunable radiation source based on an optical parametric oscillator (OPO) with a periodically poled lithium niobate (PPLN), generating light with a wavelength of ~2.1 μm in a near-degenerate regime, is developed. The use of a volume Bragg grating (VBG) as a selective element makes it possible to reduce significantly (by a factor of more than 180) the radiation linewidth. Wavelength tuning from 2050 to 2117 nm for the signal wave and from 2140 to 2208 nm for the idler wave is demonstrated. The maximum average OPO output power is found to be 617 mW (123 μJ), which corresponds to a conversion efficiency of 10%. The use of a VBG provides a fundamental possibility of designing a pump source with a small linewidth (of no more than 1 nm) and smooth wavelength tuning in a desired range for frequency converters based on non-oxide nonlinear crystals generating mid-IR light (5–15 μm).**

Keywords: *optical parametric oscillator, periodically poled nonlinear crystals, volume Bragg grating.*

1. Introduction

Radiation sources tunable in the spectral range of 5–15 μm are of interest for medical diagnostics [1], laser surgery [2], environmental monitoring [3], spectroscopy, and gas analysis [4, 5]. Currently, there are a number of promising non-oxide nonlinear crystals, such as $ZnGeP_2$, $AgGaSe_2$, $BaGa_2GeSe_6$, and OPGaAs, which possess high nonlinearity [6, 7]. However, optical parametric oscillators (OPOs) based on these crystals cannot be pumped by widespread Nd:YAG/Nd:YLF lasers with a wavelength of 1 μm because of two-photon absorption; hence, longer wavelength pump sources must be applied in this case. These are Ho:YAG lasers with a wavelength of 2.1 μm [8, 9] or, as an alternative, a cascade OPO pump setup. In the latter case, the first cascade includes an OPO based on oxide crystals, pumped by Nd:YAG/Nd:YLF lasers, and the signal or idler wave plays the role of a pump wave for the second cascade, containing a non-oxide crystal, in which generation in the spectral range of 5–15 μm occurs [10, 11]. The degenerate regime, in which the signal and idler wavelengths are either equal or close, can be used to increase the conversion efficiency of the first cascade. A drawback of this approach is the wide spectral line of output radiation, which may reach several tens or even several hundreds of nanometres. Therefore, to narrow the spectral line, one must apply additionally selective elements: Fabry–Perot etalon [12], prisms and diffraction gratings [13], or volume Bragg gratings (VBGs) [14].

A VBG was applied for the first time to narrow the emission line of an OPO based on a PPKTP crystal in 2005 [15]. The second harmonic (532 nm) of a Nd:YAG laser served as a pump wave in that study. A conversion efficiency of 35% was achieved; the corresponding linewidth of the signal wave (975 nm) was 0.16 nm. A PPKTP-based OPO with a VBG operating in a near-degenerate regime and generating radiation with a fixed wavelength of 2.13 μm and a linewidth of 2 nm was described in [16]. This source was used to pump an OPO based on a $ZnGeP_2$ crystal. In [17], a PPKTP-based OPO with a VBG, having a wavelength of ~2.1 μm and a spectral linewidth of 0.56 nm, played the role of an input signal source for subsequent amplification in two PPKTP crystals. This approach provided an output energy level of 52 mJ at pump energy of 140 mJ and a pulse repetition rate of 100 Hz.

The purpose of this study was to design a narrowband radiation source based on an OPO with a MgO:PPLN crystal, having a tuning range of more than 100 nm in the vicinity of 2.1 μm. The possibility of smooth tuning of the pump radiation wavelength, in contrast to the case of Ho:YAG laser with discretely tunable frequency, allows one to choose more efficiently appropriate conditions for further radiation conversion into the mid-IR range without resorting to angular tuning of the second-cascade OPO wavelength, which, in turn, should provide a more uniform wavelength dependence of the output radiation energy.

2. Experimental setup

An experimental setup was developed for an OPO generating in a near-degenerate mode; its schematic is presented in Fig. 1.

The pump source was a Nd:YAG laser (Canlas Laser Processing GmbH), generating 8-ns pulses with a repetition rate of 5 kHz and a wavelength of 1064 nm. The pump linewidth was measured by a High Finesse spectrometer (LSA IR-I) with a resolution of 12 GHz (~50 pm) to be 230 pm. The laser beam quality factor was $M^2 = 1.2$. Smooth control of the radiation power without changing the pulse duration and beam size was performed by a software-controlled attenuator built-in in the laser emitter. An optical Faraday isolator (*I*) was applied to prevent the radiation reflected from other

N.Yu. Kostyukova, E.Yu. Erushin, A.A. Boyko, D.B. Kolker
Novosibirsk State University, ul. Pirogova 1, 630090 Novosibirsk, Russia; e-mail: n.duhovnikova@gmail.com

Received 19 October 2021
Kvantovaya Elektronika **52** (2) 144–148 (2022)
Translated by Yu.P. Sin'kov

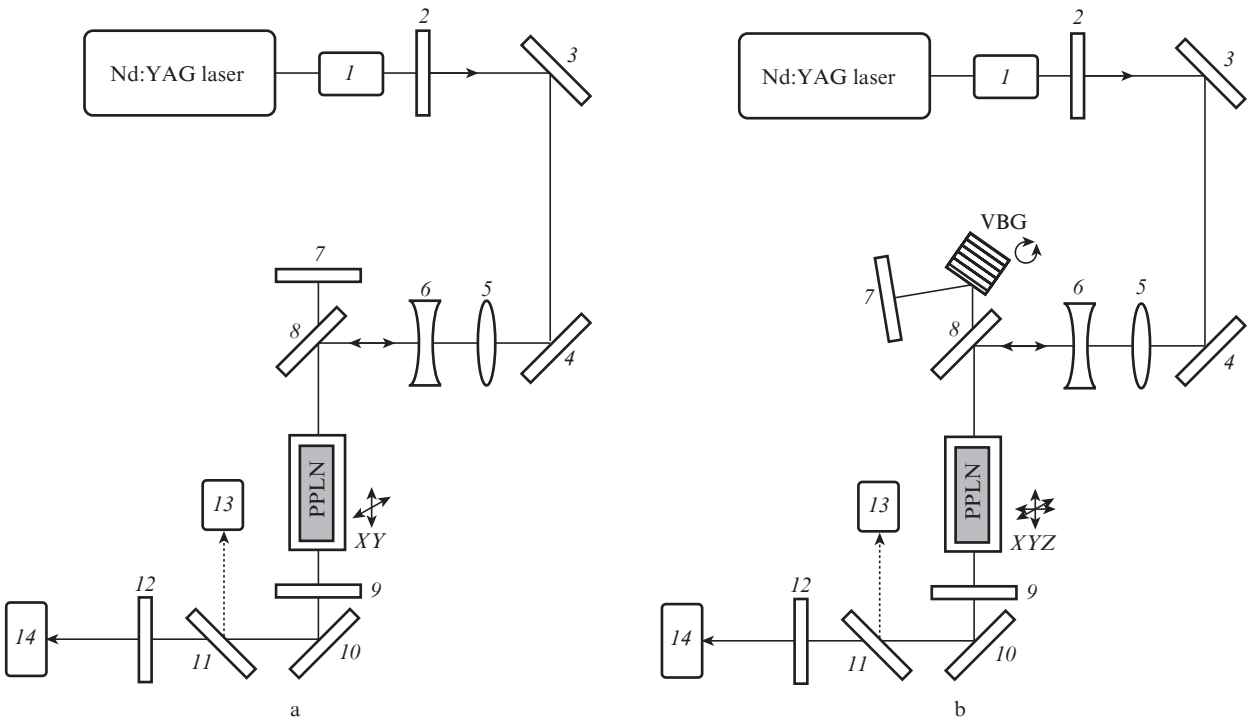

Figure 1. Schematics of the experimental setups (a) without and (b) with a VBG:
(*1*) optical Faraday isolator; (*2*) half-wave plate; (*3*, *4*, *10*) reflecting mirrors; (*5*, *6*) lenses; (*7*) OPO cavity mirror; (*8*, *11*) dielectric mirrors; (*9*) OPO cavity output mirror; (*12*) filter; (*13*) beam dump; (*14*) detector; (PPLN) MgO:PPLN crystal.

optical elements of the scheme from returning to the output laser window. A half-wave plate (*2*) provided radiation polarisation necessary for parametric frequency conversion.

Reflecting mirrors (*3*, *4*, and *10*) were used to introduce the laser beam into the OPO cavity and extract generated radiation from the cavity. System of lenses (*5* and *6*) with focal lengths $f_1 = 174$ mm and $f_2 = -100$ mm provided desired beam sizes in the crystal: $d_x = 1.3$ mm and $d_y = 1.5$ mm (at a level of e^{-2}), with a full divergence angle of ~0.4 mrad. A dielectric mirror (*8*) had a high reflectance for pump radiation, HR(45°, 1064 nm) = 99.9%, and a high transmittance for the OPO radiation, HT(45°, 2100–2150 nm) = 95%. A reflecting mirror (*7*) had a high reflectance for radiation with a wavelength of ~2.1 μm, HR(0°, 2050–2200 nm) > 97%, and mirror *9*, which served an output mirror of OPO cavity, had a high reflectance for the pump radiation, HR(0°, 1064 nm) > 99.5%, and a partial reflectance for the OPO radiation, PR(0°, 2050–2200 nm) = 60%.

Parametric frequency conversion occurs in a MgO:PPLN crystal (Labfer Ltd., Russia) 2 × 2 × 20 mm in size with a domain structure period of 32.3 μm. Antireflection coatings with HT(0°, 1064 nm) = 99% and HT(0°, 2100–2200 nm) = 98% were deposited on the crystal end faces to minimise the cavity loss. The crystal was located in a thermostat (HC Photonics Corp.), positioned on an adjusting platform with a linear mount.

In the case of OPO without a VBG, the cavity (~51 mm long) was formed by mirrors *7* and *9* (Fig. 1a). A VBG was introduced into the OPO cavity to narrow the spectral line (Fig. 1b). The OPO cavity length did not change for the light incident normally on the VBG. However, the grating was rotated to convert the OPO wavelength; in this case, the cavity length increased to ~80 mm. A VBG 5 × 5 × 5 mm in size was designed (ITMO University and SC LLS) to narrow the emission line with a wavelength of 2.117 μm for normally incident light. To minimise the optical loss in the cavity, an antireflection coating with HT(0°, 2000–2200 nm) > 97% was deposited on both grating end faces.

The OPO output radiation was directed [using a folding reflecting mirror (*10*)] to the receiving head of a power meter (*14*) (12A, Ophir). Additional separation of the signal and idler waves from the pump wave was performed using a dielectric mirror (*11*), which had a high reflectance for pump radiation, HR(45°, 1064 nm) = 99.9%, and high transmittance for generated radiation, HT(45°, 2050–2200 nm) = 92%, as well as a filter (*12*), which transmitted only radiation with a wavelength above 1.5 μm. Mirror *11* transmits radiation with a wavelength ~2.1 μm and reflects the pump radiation to a pump dump (*13*).

3. Experimental results and conclusions

3.1. Spectral characteristics

In the case of OPO, a secondary process occurring in periodically poled nonlinear crystals is the generation of the sum frequency, when the signal or idler wave interacts with the pump wave. Measuring the wavelength corresponding to the sum frequency, one can calculate the signal and idler wavelengths from the formula

$$\lambda_{s,id} = 1/\left(\frac{1}{\lambda_{meas}} - \frac{1}{\lambda_p}\right), \quad (1)$$

where λ_{meas} is the measured wavelength; $\lambda_{s,id}$ is the OPO signal, idler wavelength; and λ_p is the pump wavelength (1064.2 nm in our case).

Figure 2a shows the emission spectra for the secondary generation of sum frequency in dependence of the crystal temperature; the corresponding OPO signal or idler wavelengths are indicated above each peak. The spectra in Fig. 2 were measured using a CCS200/M Thorlabs spectrometer with a resolution of 2 nm, which replaced power meter *14* in the experimental scheme. Filter *12* was removed. One can see in Fig. 2a that the degenerate regime of OPO generation corresponds to a temperature of 67 °C.

The sum frequency generation spectra at different VBG rotation angles are shown in Fig. 2b; the corresponding OPO signal or idler wavelengths are indicated above each peak. The spectral peaks lying in the ranges of 2045–2117 and 2139–2209 nm correspond, respectively, to the signal and idler waves. At a significant VBG rotation (more than 20° with respect to the normal), the crystal temperature was reduced to 62 °C in order to increase the output power. As can be seen in Fig. 2, the output radiation spectral line obtained with the use of a VBG is much narrower than in the scheme without a VBG.

The spectral characteristics of OPO output radiation at different VBG rotation angles were studied additionally using a WS6 wavelength meter (HighFinesse/Angstrom) with a spectral resolution of 3 pm (200 MHz). Figure 3 shows software screenshots of the WS6 wavelength meter. This meter is based on a Fizeau interferometer; the recorded interference pattern is projected on a CCD line array. The values of array pixels are plotted on the horizontal axes in the screenshots, and the intensities of interference maxima are plotted on the vertical axes; panels (a, c) and (b, d) correspond to signal and idler waves, respectively.

Figures 2b and 3 demonstrate a possibility of tuning the output radiation wavelength in a wide spectral range: from 2050 to 2117 nm for the signal wave and from 2140 to 2208 nm for the idler wave. Unfortunately, the WS6 wavelength meter does not make it possible to measure directly the spectral linewidth of the output radiation. Therefore, the OPO output radiation linewidth was estimated using the scheme presented in Fig. 4.

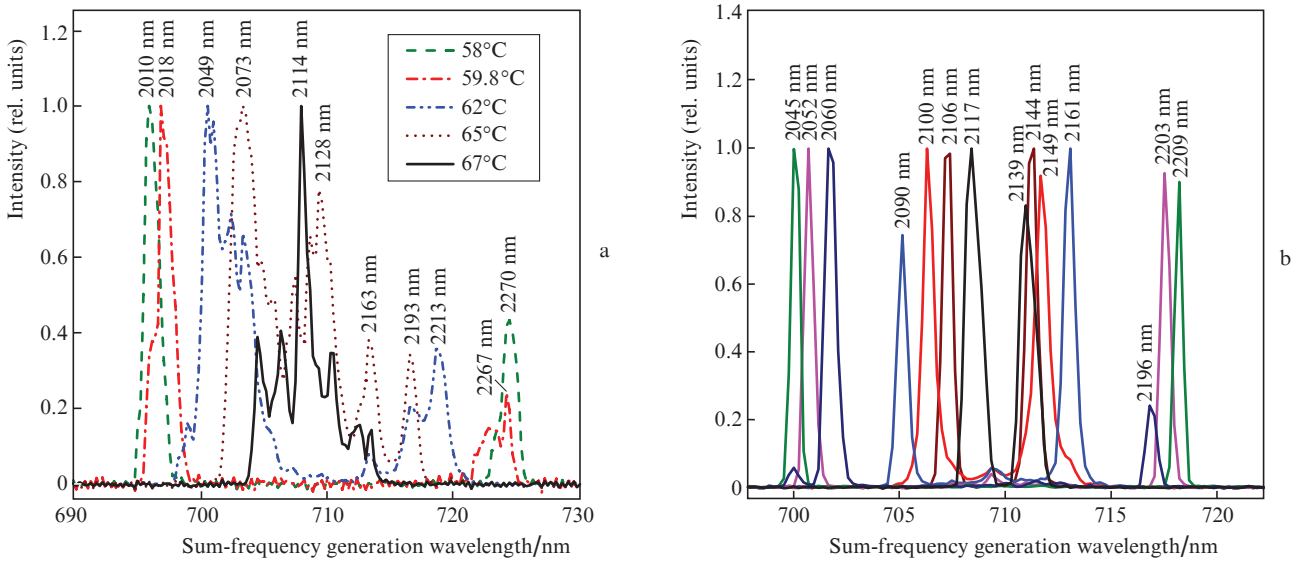

Figure 2. (Colour online) Sum frequency emission spectra, recorded (a) without a VBG at different PPLN crystal temperatures and (b) with a VBG rotated by different angles (from 0° to 24°), at fixed crystal temperatures of 67 and 62 °C (three extreme peaks at both sides in panel (b).

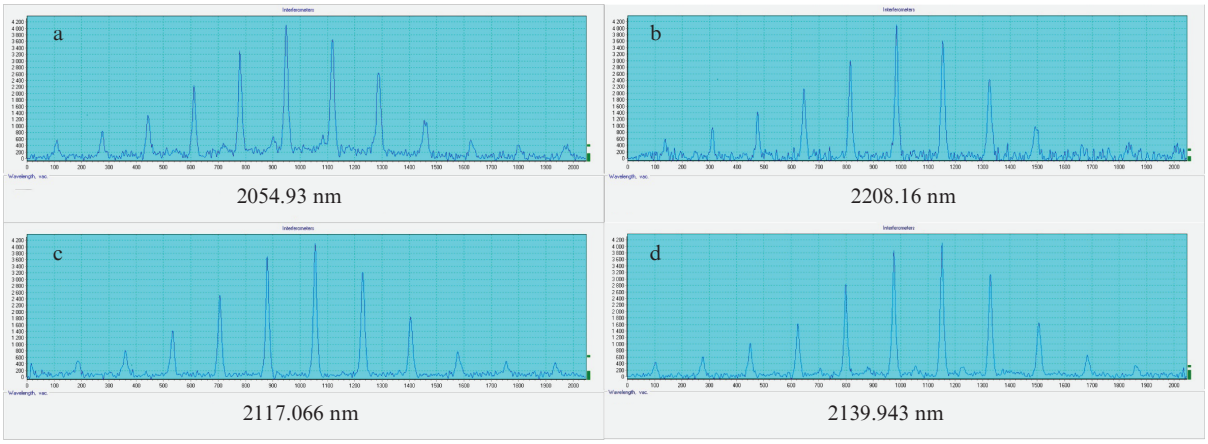

Figure 3. (Colour online) Measured output radiation wavelengths for the OPO with a VBG: (a, c) signal and (b, d) idler waves.

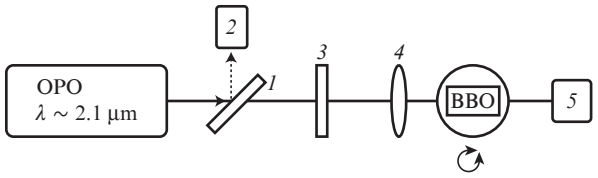

Figure 4. Schematic of the experimental setup for estimating the OPO output radiation linewidth:
(*1*) dielectric mirror; (*2*) beam dump; (*3*) filter; (*4*) lens; (*5*) High Finesse spectrometer.

A dichroic mirror (*1*) directed the OPO pump laser radiation to a beam dump (*2*), and a filter (*3*) transmitted only the radiation with a wavelength exceeding 1.5 μm, blocking the pump radiation (1.064 μm) and the sum frequency (~710 nm). Then the radiation with a wavelength of ~2.1 μm was focused by a lens (*4*) (f = 200 mm) in a 10-mm-long BBO crystal, having an aperture of 5 × 5 mm and cut angles $\varphi = 90°$ and $\theta = 22°$. The crystal was used to generate the second harmonic of output radiation. The angular phase-matching width $\Delta\theta$ was calculated (based on the dispersion relation from [18]) to be 0.063° (1.1 mrad) for the chosen interaction type (oo–e). To provide phase matching tuning, the BBO crystal was installed on a precise rotation mount (Thorlabs), providing a step of 2.4 arcmin. Then the radiation was introduced into the collimator of High Finesse spectrometer (LSA IR), which allows one to measure the radiation wavelength and linewidth in a spectral range of 800–1700 nm with a resolution of 12 GHz, which corresponds to 45 pm at a wavelength of ~1 μm.

To estimate the spectral linewidth for the OPO without a VBG, the temperature of PPLN crystal was set at a level of 67 °C; the BBO crystal was precisely rotated relative to the incident beam, which provided scanning of phase-matching angles in the crystal. The spectral measurements made it possible to estimate the output radiation linewidth for the OPO without a VBG at a level of 180 nm (Fig. 5a).

When carrying out spectral measurements to estimate the linewidth for the OPO with a VBG, the PPLN crystal temperature was maintained at the same level. The VBG position was fixed, and the phase-matching angle was scanned in the BBO crystal; this procedure was repeated for different VBG rotation angles. The OPO linewidth was varied from 400 to 550 pm (Fig. 5b). As can be seen in Fig. 5, the output radiation linewidth was significantly reduced.

3.2. Energy characteristics

Figure 6 shows the dependences of the average OPO output power on the average pump power. The generation threshold for the OPO without VBG was 0.0135 J cm^{-2} (1.5 MW cm^{-2}). The maximum average OPO output power was 1.17 W (234 μJ), and the maximum conversion efficiency reached 29.2% at a pump power of 3 W.

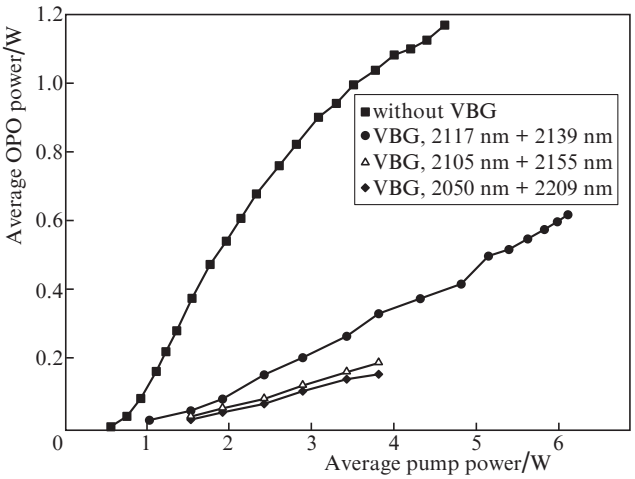

Figure 6. Dependences of the average OPO output power and conversion efficiency on the average pump power for the OPO without a VBG (squares); OPO with a VBG and normally incident beam, λ_s = 2117 nm, λ_{id} = 2139 nm (circles); OPO with a VBG and beam incident at some angle, λ_s = 2105 nm, λ_{id} = 2155 nm (triangles); and OPO with a VBG and beam incident at some angle, λ_s = 2050 nm, λ_{id} = 2209 nm (diamonds).

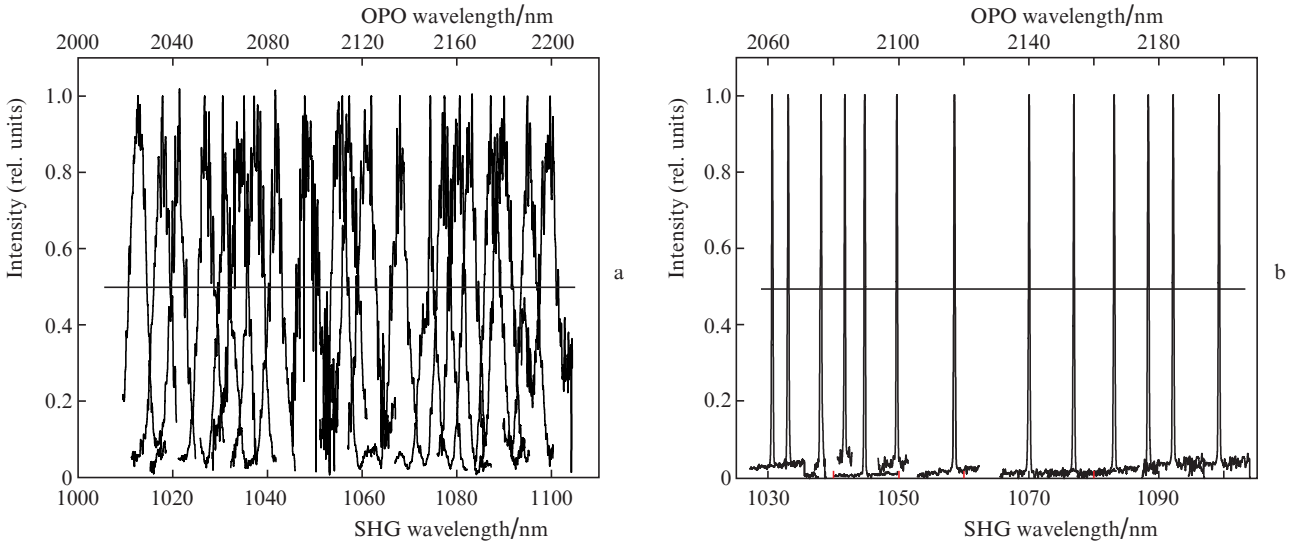

Figure 5. SHG spectra of BBO for OPOs (a) without a VBG and (b) with a VBG rotated by different angles.

The maximum average output power of the OPO with a VBG oriented normally to the beam direction was 617 mW (123 μJ). The maximum conversion efficiency at a pump power of 6.13 W reached 10%, which corresponds to a quantum efficiency of 20% and a differential efficiency of 12%. It can be seen in Fig. 6 that the output power for a beam normally incident on the VBG is twice as high as in the case of VBG oriented at some angle. This circumstance is due, in particular, to the difference in the cavity lengths in these configurations.

3.3. Spatial characteristics

The values of output beam divergence, measured using a camera of Pyrocam IV profilometer (Ophir), barely differ for the OPOs without and with VBG. In the former case the half-divergence angles along the X and Y axes were 2.62 and 3.3 mrad, respectively. The half-divergence angles for the OPO with a VBG (oriented normally) along the X and Y axes were 2.58 and 3.22 mrad, respectively. Figure 7 shows the 2D and 3D profiles of the output beam for the OPO with a VBG oriented normally to the cavity axis.

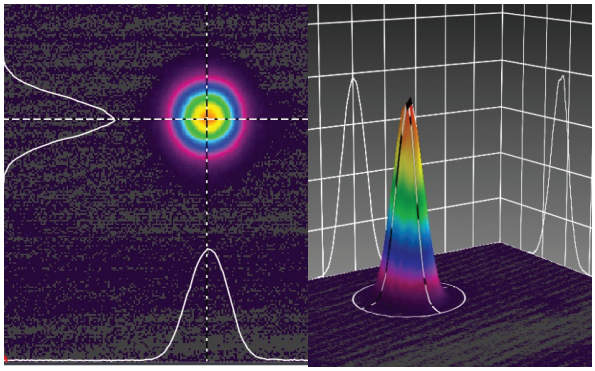

Figure 7. (Colour online) 2D and 3D beam profiles for the OPO with a VBG oriented normally to the cavity axis, at a pump power of 2 W.

4. Conclusions

In this paper, we reported the results of designing a tunable radiation source with a wavelength of ~2.1 μm, based on an OPO with a PPLN crystal, whose operation regime is close to degenerate. The maximum average OPO power, obtained without narrowing the spectral line, turned out to be 1.17 W; the beam linewidth was estimated to be ~180 nm. The introduction of a VBG into the OPO cavity provided a maximum average output power of 617 mW and demonstrated conversion of output radiation wavelength in a wide spectral range: 2050–2117 nm for the signal wave and 2140–2208 nm for the idler wave. The output radiation linewidth varied from 400 to 550 pm at different VBG rotation angles. The possibility of smooth tuning of the pump wavelength, in contrast to the discrete tuning in the case of Ho:YAG laser, allows one to choose more efficiently appropriate conditions for further wavelength conversion into the mid-IR range. Radiation sources tunable in the mid-IR range are called for to solve various gas analysis problems, including gas analysis in medical and industrial applications.

Acknowledgements. This work was supported by the Russian Science Foundation (Project no. 20-72-00032).

References

1. Kistenev Y.V., Borisov A.V., Kuzmin D.A., Penkova O.V., Kostyukova N.Y., Karapuzikov A.A. *J. Biomed. Opt*., **22**, 017002 (2017).
2. Serebryakov V.A., Boĭko É.V., Petrishchev N.N., et al. *Opt. Technol*., **77**, 6 (2010).
3. Targ R., Kavaya M.J., Huffaker R.M., Bowles R.L. *Appl. Opt*., **30**, 2013 (1991).
4. Stepanov E.V. *Tr. Inst. Obshch. Fiz. im. A. M. Prokhorova, Ross. Akad. Nauk*, **61**, 5 (2005).
5. Karapuzikov A.A., Sherstov I.V., Kolker D.B., et al. *Phys. Wave Phenom*., **22**, 189, (2014).
6. Vodopyanov K.L. *Mid-IR by Nonlinear Optical Frequency Conversion*; in *Laser-based Mid-infrared Sources and Applications* (John Wiley & Sons, 2020).
7. Badikov V.V., Badikov D.V., Laptev V.B., et al. *Opt. Mater. Express*., **6**, 2933 (2016).
8. Schunemann P.G., Zawilski K.T., Pomeranz L.A., Creeden D.J., Budni P.A. *J. Opt. Soc. Am. B*, **33**, D36 (2016).
9. Antipov O.L., Eranov I.D., Kositsyn R.I. *Quantum Electron*., **47**, 601 (2017) [*Kvantovaya Elektron*., **47**, 601 (2017)].
10. Boyko A.A., Marchev G.M., Petrov V., Pasiskevicius V., Kolker D.B., Zukauskas A., Kostyukova N.Y. *Opt. Express*., **23**, 33460 (2015).
11. Cheung E., Palese S., Injeyan H., Hoefer C., Ho J., Hilyard R., Komine H., Berg J., Bosenberg W. *Advanc. Sol. State Lasers*, **26**, WC1 (1999).
12. Vodopyanov K.L., Levi O., Kuo P.S., Pinguet T.J., Harris J.S., Fejer M.M., Gerard B., Becouarn L., Lallier E. *Opt. Lett*. **29**, 1912 (2004).
13. Nandy B., Kumar S.Ch., Casals J.C., Ye H., Ebrahim-Zadeh M.J. *Opt. Soc. Am. B*, **35**, C57 (2018).
14. Henriksson M. Doctoral Thesis *Tandem Optical Parametric Oscillators Using Volume Bragg Grating Spectral Control* (Sweden, 2010).
15. Jacobsson B., Tiihonen M., Pasiskevicius V., Laurell F. *Opt. Lett*., **30**, 2281 (2005).
16. Henriksson M., Tiihonen M., Pasiskevicius V., et al. *Appl. Phys. B*, **88**, 37 (2007).
17. Coetzee R.S., Zheng X., Fregnani L., et al. *Appl. Phys. B*, **124**, 124 (2018).
18. Kato K. *IEEE J. Quantum Electron*., **22**, 1013 (1986).